A New Dynamical Subgrid Model for the Planetary Surface Layer. Part II: Analytical Computation of Fluxes, Mean Profiles, and Variances

BERENGERE DUBRULLE

NCAR, Boulder, Colorado, and CNRS, Observatoire Midi-Pyrénées, Toulouse, France

JEAN-PHILIPPE LAVAL

NCAR, Boulder, Colorado, and SAp/DAPNIA/DSM/CEA, Gif sur Yvette, France

PETER P. SULLIVAN

NCAR, Boulder, Colorado

(Manuscript received 20 September 1999, in final form 26 January 2001)

ABSTRACT

A new dynamical subgrid model for turbulent flow is used to derive the structure of the heat and momentum fluxes, mean wind and temperature profiles, and temperature and velocity variances, as a function of the Richardson number, in the surface layer of the planetary boundary layer. Analytical solutions are obtained for stationary, homogeneous surface layers and are compared with field observations. The theory allows for analytic nonperturbative solutions in any turbulent surface layer and can be generalized in a straightforward fashion to include other effects, for example, rotation, and thus could potentially be used to estimate momentum and temperature fluxes in the planetary boundary layer for larger-scale (e.g., climate) models.

1. Introduction

In Part I of this study, Dubrulle et al. (2002, hereafter referred to as DLSW), we developed a new subgrid scale model for the surface layer of the planetary boundary layer (we refer to this as the planetary surface layer, the PSL). The complete large-eddy simulation (LES) model described in DLSW couples resolved and subgrid scales (SGS) through two dynamical equations. The SGS tensors appearing in the resolved-scale equation are computed using subgrid velocities that evolve according to a linear inhomogeneous equation; the latter is derived from the basic equations of motion under the assumption of nonlocality of the interactions at small scales.[1] In DLSW, we stress that without further approximation, the complete LES model is parameter-free, but can only be solved via a numerical implementation of both the resolved and small-scale equations. Before attempting such a computation however, we would like to present a preliminary validation of our model, where some analytical results are compared to field observations. These analytical solutions are obtained from a simplified version of the complete LES model in DLSW using three main approximations. We first assume that our surface layer is two-dimensional, that is, that both the large and the small scales vary only in the x–z plane. This approximation greatly simplifies analytical computations and does not seem to influence the mean structure of a stratified shear layer: Nazarenko (2000) has shown that the two-dimensional approximation yields the same results as the three-dimensional case (Nazarenko et al. 2000; Dubrulle et al. 2001 hereafter DLNK) for neutral surface layers, and Werne (1993) has shown that 2D convective layers exhibit behavior similar to their 3D counterparts, including transition from the soft to hard turbulence regime, that is, where the exponent of the Rayleigh versus Nusselt power law changes from 1/3 to 2/7. In the present work, we adopt the 2D approximation as a preliminary test of our modeling, leaving more detailed, 3D computations for further study. Our second assumption will be to replace the terms describing the creation of small scales via energy and heat cascades, a somewhat internal mechanism of complicated structure, by an external force, with prescribed, simple statistics. The physical idea behind this is to

[1] In this context nonlocality means we are assuming that the small scales are primarily forced by the large scales and thus we neglect nonlinear products of small-scale quantities in the subgrid velocity equations.

Corresponding author address: Dr. Peter P. Sullivan, NCAR, P.O. Box 3000, Boulder, CO 80307-3000.
E-mail: pps@ncar.ucar.edu

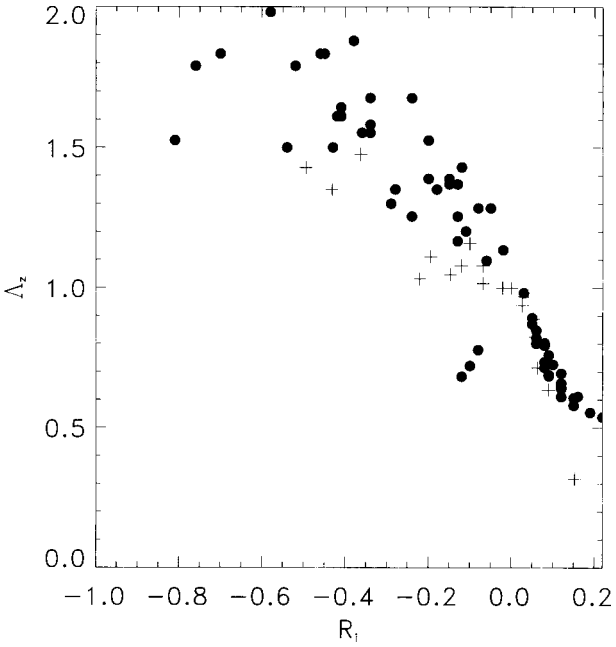

FIG. 1. Comparison of the length scale estimated by $\Lambda_z = 0.5 + 0.4/\phi_\theta$ (our theory, filled circles) and the length scale from the Kansas observations (crosses) (Wyngaard and Coté 1971).

model a posteriori the seeding of small scales by strong, intermittent plumes or streaks, detaching from the surface and propagating into the surface layer region. This idea was already used in previous work (Nazarenko et al. 2000; DLNK). Our last approximation will be to adopt a shearlike geometry in the PSL. This means that we will choose our filter defining the large and small scale, so as to keep only horizontal velocities at large scale. In the stable case, this is not too severe an approximation, since stratification precludes the existence of large-scale organized motion. In the unstable case, this approximation is justified by the fact that we consider only the area of the surface layer close to the ground. At these scales, the effect of large-scale convective motions is a large-scale sweeping movement, which occurs mainly in horizontal directions. This kind of geometry is generally accepted as representative of Boussinesq convection close to the bottom boundary (or surface) (Dubrulle 2000).

An overview of our plan of attack is as follows: simplify the full LES equations of DLSW by introducing the above assumptions (and some smaller approximations to follow) so that we can first decouple the equation for small-scale motions from the resolved field. Then owing to the linearity of the small-scale equation, it is possible to find analytic solutions. The resulting SGS fluxes are then back substituted into the resolved equations and predictions of the variation of the mean velocity and temperature profiles are deduced. Solutions of the small-scale equation can also be used to predict the variation of the turbulent flux and variance profiles. The outline of the paper is as follows; in section 2, we first derive the equations of the reduced model using the two approximations mentioned above. Analytical solutions are given in section 3 along with a comparison of the theoretical findings with observational data in section 4.

2. The ensemble-averaged equations

The equations describing the behavior of the mean temperature and velocity profiles are derived from the basic equations of the full LES model in DLSW using temporal and horizontal averaging. This averaging is achieved within our formalism by taking constant filter functions in the horizontal direction (i.e., $G_1(x) = 1/L_x$, where L_x is the horizontal scale over which the horizontal average is performed).

Also, in the development that follows, we restrict ourselves to the case where the filtering procedure retains only horizontal motions at the resolved scale. This is made possible at each level of the PSL because of the locality of the Gabor filtering procedure, which allows us to track spatially turbulent motions. Also, for a given stability state, height, and mean horizontal velocity, the peak of the vertical velocity fluctuations is shifted toward higher frequencies by about one order of magnitude with respect to the peak frequency of horizontal velocity or temperature (Kaimal et al. 1972). So, if the cutoff scale is in between the peaks of the horizontal and vertical velocity, we obtain a situation where $\langle U_i \rangle = [\langle U \rangle(z), 0, 0]$ is a horizontally homogeneous average resolved velocity, and the flow geometry becomes plane parallel. A further simplification with this choice of filtering occurs, because terms involving the large-scale vertical velocity are much smaller than the equivalent term involving the subgrid vertical velocity (e.g., $\langle \overline{U}W \rangle \ll \langle \overline{Uw} \rangle$).[2] This leads us to neglect any term involving large-scale vertical motions W in the resolved equations. Invoking the above assumptions, the dynamical equations [DLSW, their Eq. (15)] for the average resolved fields simplify to

$$\begin{aligned} \partial_z \langle \overline{Uw} \rangle + \partial_z \langle \overline{uw} \rangle &= \Delta P_* + \nu \partial_z^2 U + \mathcal{S}_1^{(u)}, \\ \partial_z \langle \overline{w^2} \rangle &= -\partial_z \langle P \rangle + g\beta(\Theta - T_0) \\ \partial_z \langle \overline{w\Theta} \rangle + \partial_z \langle \overline{w\theta} \rangle &= -\partial_t \langle \Theta \rangle + \kappa \partial_z^2 \Theta + \mathcal{S}^{(\theta)}. \end{aligned} \quad (1)$$

Notice that in the u momentum equation we have included a nonzero pressure gradient ΔP_* that serves as the primary shear forcing. Recall that the x coordinate is taken to be aligned with the average surface layer wind (see section 3a), and thus in the context of the atmospheric boundary layer ΔP_* is related to the large-scale geostrophic wind, that is, $\Delta P_* = -fV_g$, where f is the Coriolis parameter and V_g is the y component of the geostrophic wind. Over the limited vertical extent

[2] Here filtered variables are indicated by $\overline{(\,)}$ and ensemble averaging by $\langle\,\rangle$, see DLSW for a definition of all symbols.

of the surface layer, we consider ΔP_* to be independent of the vertical coordinate z.

In our full LES model, the subgrid velocity and temperature are governed by generalized rapid distortion equations [DLSW, their Eq. (18)]. If we apply the same parallel flow assumptions to these small-scale equations they can be transformed into the set of ray equations

$$D_t x = \langle U \rangle, \qquad D_t z = 0, \qquad D_t k = 0,$$
$$D_t q = -k\partial_z \langle U \rangle, \tag{2}$$

where the advective operator $D_t = \partial_t + \langle U \rangle \partial_x - k\partial_z \langle U \rangle \partial_q$, and (k, q) denote components of the wavenumber vector. Integration of (2) with respect to time is straightforward in this shear flow case and yields

$$x = (t - t_0)\langle U \rangle + x_0, \qquad z = z_0, \qquad k = k_0,$$
$$q = q_0 - k(t - t_0)\partial_z \langle U \rangle, \tag{3}$$

where x_0, z_0, k_0, and q_0 are the initial conditions of the particular ray under consideration. This equation shows that the parameter $R = q/k$ can be used as a surrogate for t to identify the trajectories. Changing variables from t to R, and taking into account the plane parallel geometry we get instead of DLSW's Eq. (20), the equations

$$D_R \hat{u} = -\frac{1 - R^2}{1 + R^2}\hat{w} + \frac{R}{1 + R^2}\frac{g\beta}{\partial_z U}\hat{\theta} + \frac{\nu k^2}{\partial_z U}(1 + R^2)\hat{u} - \frac{1}{\partial_z U}\hat{F}_u^{\perp},$$
$$D_R \hat{w} = -\frac{2R}{1 + R^2}\hat{w} - \frac{1}{1 + R^2}\frac{g\beta}{\partial_z U}\hat{\theta} + \frac{\nu k^2}{\partial_z U}(1 + R^2)\hat{w} - \frac{1}{\partial_z U}\hat{F}_w^{\perp},$$
$$D_R \hat{\theta} = +\hat{w}\frac{\partial_z \Theta}{\partial z U} + \frac{\kappa k^2}{\partial_z U}(1 + R^2)\hat{\theta} - \frac{1}{\partial_z U}\hat{F}_\theta. \tag{4}$$

We now use our second assumption to simplify the system: from now on, we consider the forces F_u, F_w, and F_θ in (4) to be externally imposed forces, with prescribed properties. The simplest choice we can make is to assume that the forces are delta correlated in space and time. Less restrictive conditions can be made that achieve the same results, but computations are more complicated. Using the delta-correlation assumption, it can be shown (DLNK) that the correlation of two forces corresponding to rays emanating from the same origin is

$$\langle \hat{F}_i^{\perp}(x, k, t)\hat{F}_j^{\perp}(x, k', t') \rangle \propto A_{ij}(k)\delta(k + k'), \tag{5}$$

where the coefficient of proportionality depends only on the mean gradients, the angle between the vector components of k, and is independent of the spatial coordinates (a property that will be used later).

3. Analytical solutions

a. Subgrid-scale solution

With prescribed external forces, the subgrid fields are just solutions of a linear inhomogeneous system. In the appendix, we show that the solution can be written as

$$(u, w, \theta)(R) = \int_{-\infty}^{R} (\tilde{u}, \tilde{w}, \tilde{\theta})(R, R_0)\, dR_0, \tag{6}$$

where $(\tilde{u}, \tilde{w}, \tilde{\theta})(R, R_0)$ are the homogeneous solutions of (4) (i.e., with no force terms), such that at $R = R_0$,

$$(\tilde{u}, \tilde{w}, \tilde{\theta})(R, R) = -\frac{1}{\partial_z U}(F_u^{\perp}, F_w^{\perp}, F_\theta)(R). \tag{7}$$

It is also shown in the appendix that because of the delta correlation of the forces, the time-averaged product $\langle \hat{u}\hat{w} \rangle$ can be written as a function of the product $\tilde{u}\tilde{w}$; that is,

$$\langle \hat{u}\hat{w} \rangle = |\partial_z U| \int_{-\infty}^{R} \langle \tilde{u}\tilde{w}(R, R_0) \rangle\, dR_0. \tag{8}$$

We can now solve the homogeneous system easily by taking the Prandtl number $\mathrm{Pr} = \nu/\kappa = 1$ (in the atmosphere $\mathrm{Pr} \approx 0.7$). Moreover, in our model, viscosity and diffusivity serve to damp out those motions that may otherwise grow unbounded (e.g., in unstable situations, see appendix). With this approximation, one can find solutions of the homogeneous system in terms of hypergeometrical functions. This is also detailed in the appendix. The corresponding solutions decay at large R, either monotonically for $R_i < 0.25$, or in an oscillatory manner for $R_i > 0.25$, where the Richardson number $R_i = g\beta\partial_z \Theta/(\partial_z U)^2$. In the surface layer, it seems that the Richardson number never exceeds 0.25; thus, the oscillatory solution is not considered any further.

To gain physical insight into the meaning of the subgrid stresses, it is interesting to consider the inviscid solution of Eq. (4), which allow an expression of the subgrid stresses without taking into account the detailed shape of the solution. Indeed, we have by definition:

$$\overline{wu} = \frac{1}{2}\int [\hat{u}(\mathbf{k}, \mathbf{x}, t)\hat{w}(-\mathbf{k}, \mathbf{x}, t) + \hat{u}(-\mathbf{k}, \mathbf{x}, t)\hat{w}(\mathbf{k}, \mathbf{x}, t)]\, d\mathbf{k},$$
$$\overline{w\theta} = \frac{1}{2}\int [\hat{w}(\mathbf{k}, \mathbf{x}, t)\hat{\theta}(-\mathbf{k}, \mathbf{x}, t) + \hat{w}(-\mathbf{k}, \mathbf{x}, t)\hat{\theta}(\mathbf{k}, \mathbf{x}, t)]\, d\mathbf{k}. \tag{9}$$

Introducing the vorticity $\hat{\omega} = iq\hat{u} - ik\hat{w}$ (see the appendix), changing from variable q into R in the integral and then interchanging the integrations between R and R_0, we then get, in terms of the tilde variables (solutions of the homogeneous system):

$$\langle \overline{wu} \rangle = |\partial_z U| \int \frac{dk}{k} \int dR_0 \int_{-\infty}^{R_0} dR \frac{R}{(1 + R^2)^2} \langle |\tilde{\omega}|^2 \rangle,$$

$$\langle \overline{w\theta} \rangle = |\partial_z U| \frac{i}{2} \int dk \int dR_0 \int_{-\infty}^{R_0} dR \frac{\langle \tilde{\omega}\tilde{\theta}^* - \tilde{\omega}^*\tilde{\theta} \rangle}{1 + R^2}, \tag{10}$$

where the asterisk denotes the complex conjugate, and we have taken advantage of the delta correlation of the forces (see appendix).

Let us now integrate by parts with respect to R the two integrals of (10). For the first one, we get, using (A2):

$$\begin{aligned} \langle \overline{wu} \rangle &= -\frac{|\partial_z U|}{2} \int \frac{dk}{k} \int dR_0 \left[\frac{\langle |\tilde{\omega}|^2 \rangle}{1 + R^2} \right]_{-\infty}^{R_0} \\ &\quad + \frac{|\partial_z U|}{2} \int \frac{dk}{k} \int dR_0 \int_{-\infty}^{R_0} dR \frac{D_R \langle |\tilde{\omega}|^2 \rangle}{1 + R^2} \\ &= \frac{\lambda(z, t)}{\partial_z U} + \frac{g\beta}{\partial_z U} \langle \overline{w\theta} \rangle, \end{aligned} \tag{11}$$

where

$$\lambda = \int d\mathbf{k} \frac{\langle |(iqF_u - ikF_w)(k, \mathbf{x}, t)|^2 \rangle}{\mathbf{k}^2} = \langle \overline{F}_u^2 + \overline{F}_w^2 \rangle$$

is a function depending on the small-scale turbulent forcing by the large scales. For $\langle \overline{w\theta} \rangle$, we again use (A2) to get

$$\begin{aligned} \langle \overline{w\theta} \rangle &= -\frac{(\partial_z U)^2}{\partial_z \Theta} \int k\, dk \int dR_0 \int_{-\infty}^{R_0} dR D_R \langle |\tilde{\theta}|^2 \rangle \\ &= -\frac{(\partial_z U)^2}{\partial_z \Theta} \int k\, dk \int dR_0 [\langle |\tilde{\theta}|^2 \rangle]_{-\infty}^{R_0} \\ &= \frac{\mu(z, t)}{\partial_z \Theta}, \end{aligned} \tag{12}$$

where

$$\mu = \int d\mathbf{k} \langle |F_\theta|^2 \rangle = \langle \overline{F}_\theta^2 \rangle$$

is a function depending on the small-scale temperature forcing by the large scale.

For $\langle \overline{Uw} \rangle$ and $\langle \overline{\Theta w} \rangle$ we proceed along the same lines using the approximation (valid to leading order in ϵ)

$$\overline{Uw} \approx U\overline{w}, \qquad \overline{\Theta w} \approx \Theta \overline{w}, \tag{13}$$

with

$$\begin{aligned} \langle U\overline{w} \rangle &= \left\langle U \frac{1}{2} \int d\mathbf{k} [\hat{1}(\mathbf{k}, \mathbf{x}, t)\hat{w}(\mathbf{x}, -\mathbf{k}, t) \right. \\ &\qquad \left. + \hat{1}(-\mathbf{k}, \mathbf{x}, t)\hat{w}(\mathbf{x}, \mathbf{k}, t)] \right\rangle \\ &= -i \int k\, dk \int dR_0 \int_{-\infty}^{R_0} dR \langle \Re(U\hat{1}\tilde{w}^*) \rangle \\ &= \frac{\partial_z U}{\partial z \Theta} \int k\, dk \int dR_0 \int_{-\infty}^{R_0} dR D_R \langle \Re(U\hat{1}\tilde{\theta}^*) \rangle \\ &= \frac{\langle U \rangle \eta(z, t)}{\partial_z \Theta}, \end{aligned} \tag{14}$$

where

$$\eta \langle U \rangle = \int d\mathbf{k} \Re \langle (U\hat{1}\hat{F}_\theta^*) \rangle.$$

Here η, μ, and λ are the only parameters in our model. They are a priori functions of both z and R_i, and are not arbitrary free parameters, but are connected with the energy and heat cascade from the large to small scales. Of course, the ''amount'' of energy or heat cascading depends upon the filter that is used, so these constants can be expected to be ''filter dependent.'' Note that in all our integrations by parts, we have neglected terms of order ν, because we have considered the inviscid limit. In reality, viscosity is nonzero, and hence serves to regularize the solutions and avoid potential divergences (Nazarenko et al. 2000). Therefore, we can expect our coefficient η, μ, and λ to depend also on the ratio $\nu/\partial_z U$ in a nontrivial way. This is explained in the appendix.

The exact value of η, μ, and λ can be obtained, in principle, from a full LES where the contributions from the subgrid scales, expressed by (11), (12), and (14), are computed self-consistently at each time step via the forces. In the present part, we stick to analytic or semianalytic computations, to study the main features of the resulting equilibrium profiles.

b. Resolved-scale solution

Substitution of the subgrid stresses (11), (12), and (13) into the resolved-scale equations (1) and neglecting terms involving the viscosity or surface terms (which are important only very close to the surface) leads to

$$\begin{aligned} \partial_z \left(\frac{\eta U}{\partial_z \Theta} + \frac{\lambda}{\partial_z U} + \frac{g\beta\mu}{\partial_z \Theta \partial_z U} \right) &= \Delta P_*, \\ \partial_z \langle w^2 \rangle &= -\partial_z \langle P \rangle + g\beta(\Theta - T_0), \\ \partial_z \left(\frac{\eta\Theta}{\partial_z \Theta} + \frac{\mu}{\partial_z \Theta} \right) &= -\langle \partial_t \Theta \rangle, \end{aligned} \tag{15}$$

where the second equation of (15) is just the expression of hydrostatic equilibrium.

We now nondimensionalize lengths by d (to be fixed later), velocities by u_*, and temperature by $\theta_* = -Q_0/u_*$. Note that λ and μ are dimensionally equivalent to an energy and heat transfer, respectively. So we may write:

$$\lambda = \frac{u_*^3}{d}\tilde{\lambda}, \qquad \mu = \frac{u_*\theta_*^2}{d}\tilde{\mu}, \tag{16}$$

where $\tilde{\lambda}$ and $\tilde{\mu}$ are nondimensional functions of $\tilde{z}$ and R_i. We stress here again that they are filter dependent, and that their exact value can be obtained via a complete LES. For the term η, we proceed along the same lines to get:

$$\eta = \frac{u_*\theta_*}{d}\tilde{\eta}, \tag{17}$$

where the tilde refers to nondimensionalized quantities, such as z/d. With this nondimensionalization, and after integration over $\tilde{z}$ of the first and the third equations of (15), the system of ordinary differential equations becomes

$$\tilde{\eta}\frac{\tilde{U}}{\partial_{\tilde{z}}\tilde{\Theta}} + \tilde{\lambda}\frac{1}{\partial_{\tilde{z}}\tilde{U}} + \tilde{\mu}\frac{1}{\partial_{\tilde{z}}\tilde{\Theta}\partial_{\tilde{z}}\tilde{U}}\frac{d}{KL} = \frac{\Delta P_*}{u_*^2}(\tilde{z} - \tilde{h}_u),$$

$$\tilde{\eta}\frac{\tilde{\Theta}}{\partial_{\tilde{z}}\tilde{\Theta}} + \tilde{\mu}\frac{1}{\partial_{\tilde{z}}\tilde{\Theta}} = \frac{\langle\partial_t\Theta\rangle}{Q_0}(\tilde{z} - \tilde{h}_\theta), \tag{18}$$

where $L = -u_*^3/Kg\beta Q_0$ is the Obukhov length, K is the von Kármán constant, and the integration constants $\tilde{h}_u$ and $\tilde{h}_\theta$ are the locations where the momentum and heat flux vanish.[3] Their value and their ratio may a priori depend on the Richardson number. Note that by taking the limit $\tilde{z} \to 0$, one can actually relate ΔP_* and $\langle\partial_t\Theta\rangle$ to u_* and Q_0. Indeed, we know that at this location, the momentum flux tends to $-u_*^2$ and the heat flux tends to Q_0. We thus get

$$\Delta P_* = \frac{u_*^2}{\tilde{h}_u}, \qquad \langle\partial_t\Theta\rangle = \frac{Q_0}{\tilde{h}_\theta}. \tag{19}$$

The set of coupled equations (18) can be used in two ways to gain information about the behavior of the solution. First, by fixing $\tilde{z}$ inside the surface layer, and then choosing $d = l_z$, the characteristic ''vertical scale'' of the motions then one can get an estimate of the behavior of l_z, which is associated with the length scale corresponding to the peak frequency of the vertical spectrum. This is done in section 4a. Second, by setting $d = L$, for example (the same for all z), we can integrate the set of coupled equations (18) as a function of z, to obtain the mean temperature and equilibrium profiles. This is done in section 4b.

4. Application

a. The vertical length scale

To get an estimate of the variation of the vertical length scale l_z at some fixed z, as a function of the stability parameter L, we consider the second equation of (18) with $d = l_z$. In the surface layer $z \ll h_\theta$, so that the rhs of the equation can be taken as equal to unity. Introducing the nondimensional lengthscale $\Lambda_z = l_z/Kz$ and the universal stability function $\phi_\theta = zK\partial_z\Theta/\theta_* = \partial_{\tilde{z}}\tilde{\Theta}/\Lambda_z$, we get an explicit equation for the nondimensional lengthscale, as

$$\Lambda_z = \frac{\tilde{\eta}\tilde{\Theta} + \tilde{\mu}}{\phi_\theta}. \tag{20}$$

We see that Λ_z is a simple function of the universal stability function ϕ_θ and of the nondimensional temperature $\tilde{\Theta}$. Considering the case where $\tilde{\eta}$ is a constant, we see that the length scale can be written as $\Lambda_z = (A\tilde{\Theta} + B)/\phi_\theta$. Figure 1 shows a comparison of this estimate with the nondimensionalized peak lengthscale measured by Wyngaard and Coté (1971) for the Kansas data as a function of the Richardson number. The temperature $\tilde{\Theta}$ has been estimated using (28). One can see that even this simple estimate reproduces quite well the behavior of the peak length scale.

b. Mean velocity and temperature profiles

In this section, we compute the equilibrium temperature and velocity profiles in the situation where l_z is fixed, and the nondimensional scale is taken as $d = L$, where L is the Monin–Obukhov length scale.

The mean velocity and temperature profiles can be found upon solving the system of equations (18) together with (19). This can be done once the z and R_i dependence of the three parameters $\tilde{\lambda}$, $\tilde{\mu}$, and $\tilde{\eta}$ is known. This dependence can be found using cumbersome asymptotic analysis, detailed in the appendix. Before presenting the details of this asymptotic analysis, we would like to make some simple, physical analysis of Eq. (18) to show that it already includes some interesting information about the profiles.

1) Qualitative analysis: Stable case

Let us first consider a stable situation, corresponding to $\zeta = z/L \gg 1$. Because of the stable stratification, one expects the vertical motions to be severely damped, even at small scales. However, correlations between vertical velocity and temperatures may still be very strong, and so one qualitatively expects that $\langle U\overline{w}\rangle \ll \langle\overline{uw}\rangle$ and $\langle\Theta\overline{w}\rangle \ll \langle\overline{\theta w}\rangle$. This means that in (18), we can keep only the contribution from $\langle uw\rangle$ and $\langle w\theta\rangle$, giving:

$$\tilde{\lambda}\frac{1}{\partial_{\tilde{z}}\tilde{U}} + \tilde{\mu}\frac{1}{\partial_{\tilde{z}}\tilde{\Theta}\partial_{\tilde{z}}\tilde{U}}\frac{1}{K} = \frac{\zeta}{\tilde{h}_u} - 1,$$

$$\tilde{\mu}\frac{1}{\partial_{\tilde{z}}\tilde{\Theta}} = \frac{\zeta}{\tilde{h}_\theta} - 1, \tag{21}$$

where we have used (19) to simplify the rhs. We know, from the previous section and from the analytic solutions of the small scales, that $\tilde{\lambda}$ only depends on $\partial_{\tilde{z}}\tilde{U}$

[3] This location is in general outside the physical definition of the surface layer, so that the fluxes usually do not vanish inside the surface layer.

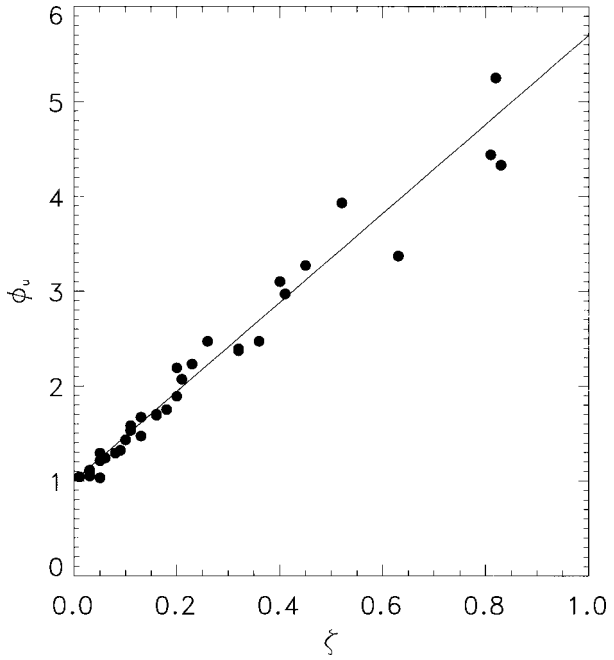

FIG. 2. Comparison between the theoretical prediction (line) given by (24) and the Kansas data (filled circles) for the stability function ϕ_u as a function of ζ in stable conditions. The slope of the line has been adjusted to give the best fit.

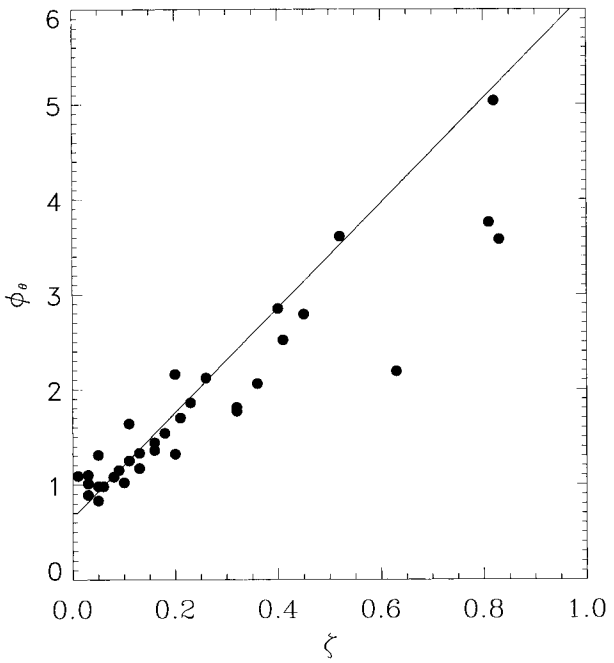

FIG. 3. Comparison between the theoretical prediction (line) given by (25) and the Kansas data (filled circles) for the stability function ϕ_θ as a function of ζ in stable conditions. The slope of the line has not been adjusted but computed using (25).

and on R_i. Actually, in the Kansas data, one observes that for stable stratification, the Richardson number tends to a constant value, very close to the critical value $R_i \to 1/4$, $\zeta \gg 1$. This suggests that in stable situations, $\tilde{\lambda}$ can be expanded as a function of $\partial_{\tilde{z}}\tilde{U}$ only

$$\tilde{\lambda} = \lambda^{(0)} + \partial_{\tilde{z}}\tilde{U}\lambda^{(1)} + \cdots. \tag{22}$$

Substitution of this expansion into the first equation of (21) and using the second equation, we then obtain the prediction for the mean nondimensional profile function $\phi_u = Kz\partial_z U/u_*$:

$$\phi_u = \frac{\zeta^2/\tilde{h}_\theta + \zeta(\lambda^{(0)}K - 1)}{\zeta/\tilde{h}_u - 1 - \lambda^{(1)}}. \tag{23}$$

In the limit $\zeta \to 0$, $\phi_u \to 1$, which suggests that $\lambda^{(1)} = -1$ and $\lambda^{(0)} = (1 + \tilde{h}_u)/(K\tilde{h}_u)$. In the stable case, we finally get the relation

$$\phi_u = 1 + \frac{h_u}{h_\theta}\zeta, \qquad \zeta > 0. \tag{24}$$

This relation is very well satisfied by the Kansas data (as shown in Fig. 2), from which we get the prediction $h_u/h_\theta \approx 4.7$. It is difficult to get a consistency check of this relation, because data on the vertical behavior of the momentum and heat flux usually display a fair amount of scatter. If we consider the measurements of Caughey et al. (1979), for example, and fit a linear expression to the fluxes (so as to get values of h_u and h_θ) values of h_θ/h_u varying between 0.3 and 0.8 are obtained. This is consistent with the value obtained from the Kansas data, which gives $1/4.7 \approx 0.22$. We may then use the value of the Richardson number $R_i \approx 1/4$ when $\zeta \gg 1$ to gain information about the nondimensional temperature profile $\phi_\theta = Kz\partial_z\Theta/\theta_*$. Indeed, since $R_i = \zeta\phi_\theta/\phi_u^2$, we have from (24):

$$\phi_\theta = \frac{1}{4}\frac{\phi_u^2}{\zeta} \approx \frac{4.7^2}{4}\zeta, \qquad \zeta \gg 1. \tag{25}$$

A patching at the neutral case, where ϕ_θ tends to a constant of the order of 0.65 suggests finally to add a constant in the rhs of (25), which then becomes

$$\phi_\theta = 0.65 + \frac{4.7^2}{4}\zeta, \qquad \zeta \gg 1. \tag{26}$$

This relation is also well satisfied by the Kansas date (Fig. 3).

2) QUALITATIVE ANALYSIS: UNSTABLE CASE

Because of the convective motions in the unstable case, we expect the subgrid stresses involving $\overline{w}$ to be dominant, at least for those stability conditions where the mean flow $\langle U\rangle$ is not yet negligible: $\langle U\overline{w}\rangle \gg \langle\overline{uw}\rangle$ and $\langle\Theta\overline{w}\rangle \gg \langle\overline{\theta w}\rangle$. This has been experimentally observed for surface layers around $\zeta = -1$ by Tong et al. (1999). In that case, from (18) and since ζ is small in front of both $\tilde{h}_u$ and $\tilde{h}_\theta$, we get the relation:

$$\frac{\tilde{\Theta}}{\tilde{U}} = 1. \tag{27}$$

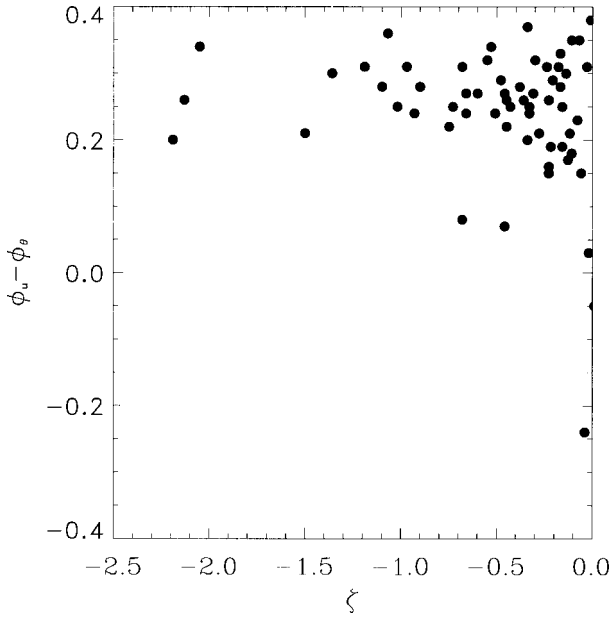

FIG. 4. Comparison of relation (29) with the Kansas data. One sees that $\phi_u - \phi_\theta$ is indeed constant over a wide range of ζ under unstable conditions.

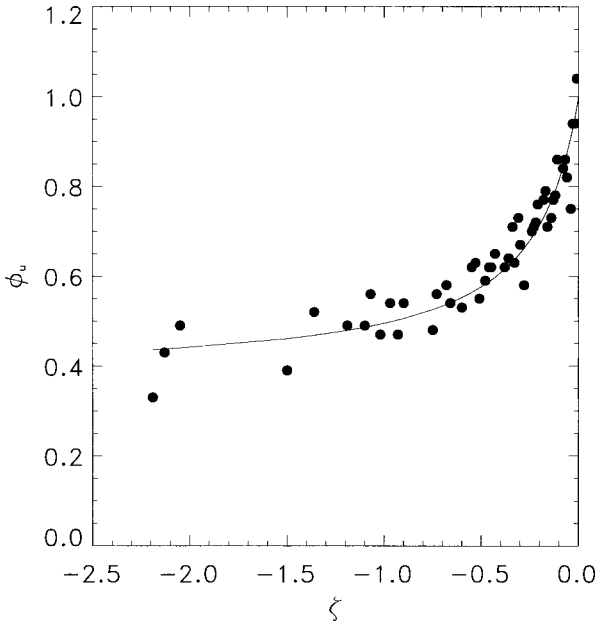

FIG. 5. Comparison of the theoretical prediction (41) (line) with the Kansas observations (filled circles) for the stability function ϕ_u under unstable conditions. The best agreement is obtained with $\alpha_2 = -1.58$ and $\alpha_3 = -4.21$.

We may then relate $\tilde{U}$ and $\tilde{\Theta}$ to the universal stability functions ϕ_θ and $\phi_u = Kz\partial_z U/u_*$ via a Taylor expansion near the bottom of the surface layer $z \approx 0$:

$$\tilde{U} = \tilde{U}_0 + z\partial_z\tilde{U} = \tilde{U}_0 + \alpha\phi_u,$$
$$\tilde{\Theta} = \tilde{\Theta}_0 + z\partial_z\tilde{\Theta} = \tilde{\Theta}_0 + \beta\phi_\theta, \qquad (28)$$

where $\alpha = \beta = 1/K$. This approximation is also valid if ϕ_u and ϕ_θ behave like power laws in ζ, in which case α and β are more generally connected to the power-law exponents. The approximation (28) encompasses two types of situations; either ϕ_u and/or ϕ_θ tends to a constant, in which case by convention, we will set $\zeta^0 = \ln(z)$, and $\tilde{U}_0$ and $\tilde{\Theta}_0$ are then just constants in the log law; or ϕ_u and/or ϕ_θ tend to zero, in which case by convention we set $\tilde{U}_0 = 0$ (thus there is only a very weak mean wind), which in turn implies $\tilde{\Theta}_0 = 0$.

Using (28) and (27), we thus get

$$\phi_u - \phi_\theta = \tilde{U}_0 - \tilde{\Theta}_0 = cte. \qquad (29)$$

This prediction is rather well satisfied by the Kansas data (as shown in Fig. 4), for $-2 < \zeta < 0$. Extrapolating to larger values of $-\zeta$, one easily checks that (29) can only be satisfied provided either ϕ_u and ϕ_θ both tend to a constant, or one of them tends to a constant, while the other one approaches zero. Given the limited range of ζ in the data (we were not able to find any data with ζ much less than -2), it is difficult to assess whether ϕ_u or ϕ_θ indeed tend to a constant value at large $-\zeta$. A partial qualitative answer can be obtained by examining the situation where the mean wind becomes negligible, and the surface subgrid stress tends to zero (which is traditionally the situation expected at $\zeta \ll -1$.

In such a case, (18) gives

$$\langle \overline{uw} \rangle \sim z, \qquad \langle \Theta\overline{w} \rangle \sim 1. \qquad (30)$$

Finally using the expressions $\langle \overline{uw} \rangle$ and $\langle \Theta\overline{w} \rangle$ derived in (15), we can express ϕ_u as

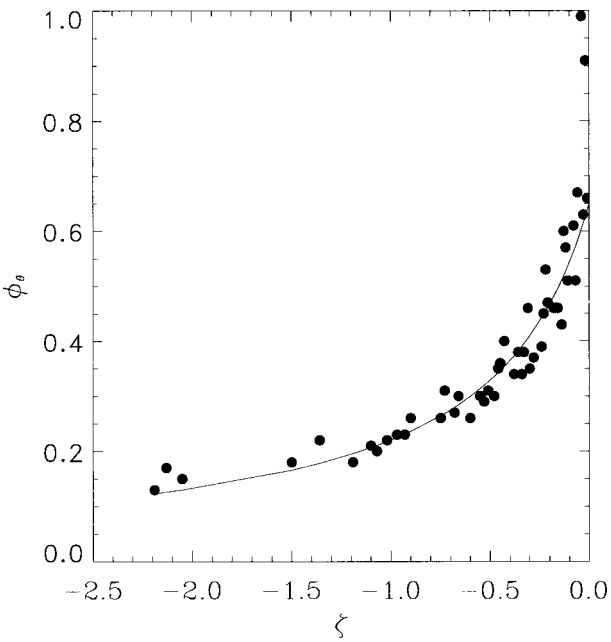

FIG. 6. Comparison of the theoretical prediction (41) (line) and the Kansas data (filled circles) for the stability function ϕ_θ under unstable conditions. The best agreement is obtained with $\beta_1 = 0.65$ and $\beta_2 = -1.95$.

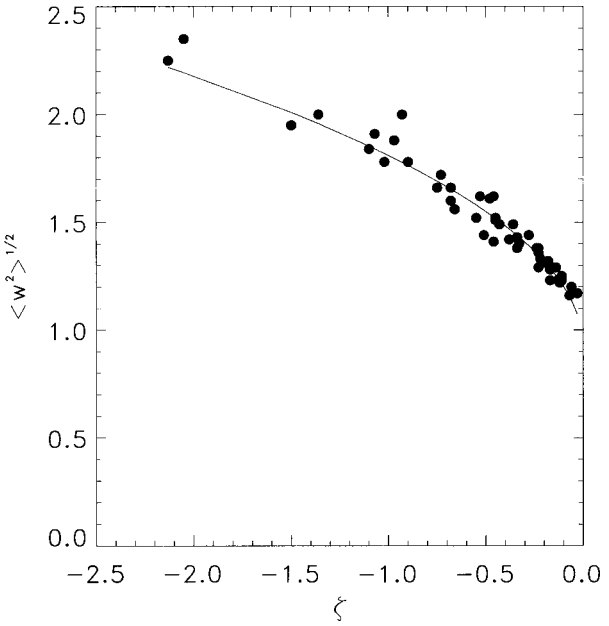

FIG. 7. Comparison of the theoretical prediction (43) (line) with the Kansas observations (filled circles) for the vertical velocity $\langle w^2\rangle^{1/2}$ under unstable conditions. The best agreement is obtained with $\alpha_1 = 0.92$ and $\alpha_2 = 0.89$.

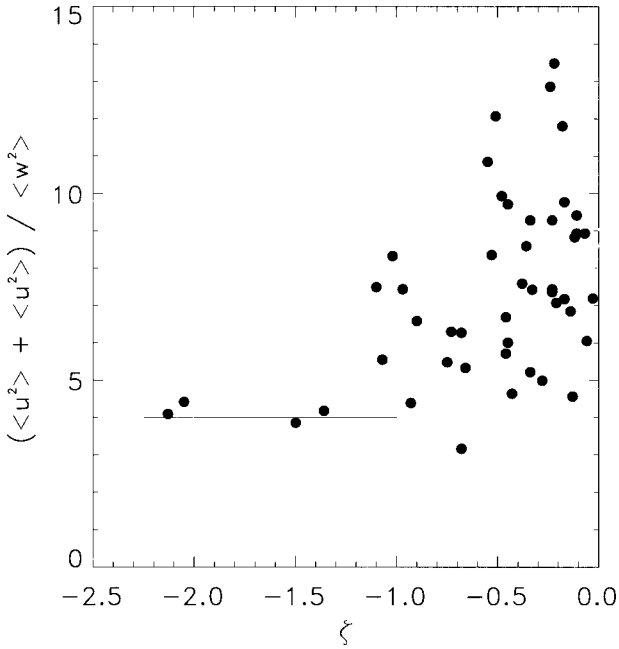

FIG. 8. Comparison of the constant theoretical prediction (line) with the Kansas observations (filled circles) for the $(\langle u^2\rangle + \langle v^2\rangle)/\langle w^2\rangle$ under unstable conditions.

$$\phi_u = \tilde{\lambda} + \frac{\tilde{\mu}}{\tilde{\eta}\tilde{\Theta}}. \tag{31}$$

At this stage, we have no information on $\tilde{\lambda}$, $\tilde{\mu}$, and $\tilde{\eta}$. We see nevertheless that by assuming a slow variation in the surface layer, we can expect from (31) that the quantity ϕ_u asymptotically approaches a constant. We shall see in the next section that this guess is actually confirmed by a more detailed asymptotic analysis.

The results obtained previously, although in good agreement with the Kansas data, are only qualitative because we used some physical hypotheses as input. In the next section, we turn to more quantitative results by using the asymptotic expansions of the subgrid-scale solution derived in the appendix.

3) Quantitative analysis: Neutral case

In the neutral case $R_i = 0$, the asymptotic behavior given in the appendix shows that $\langle\overline{w}\rangle$, $\langle\overline{uw}\rangle$, and $\langle\overline{u\theta}\rangle$ all behave like $1/\partial_z U$ with a proportionality factor that is a function of $\partial_z U$ via the viscous damping. This case has been studied in detail in the 2D case in Nazarenko (2000), and in the 3D case in Nazarenko et al. (2000) and DLNK. We sketch here the main findings of these studies. Given the functional form:

$$\langle U\overline{w}\rangle = \frac{\eta\langle U\rangle}{\partial_z U}, \qquad \langle\overline{uw}\rangle = \frac{\lambda}{\partial_z U},$$

$$\langle\overline{w\theta}\rangle = \frac{\mu}{\partial_z U}. \tag{32}$$

The functions λ, η, and μ are dependent on z only through $\partial_z U$, and thus can be expanded near the surface in terms of $\partial_z U - u_*^2/\nu$. The condition that the turbulent stress is zero at the wall imposes the condition $\lambda/\lambda_0 = \mu/\mu_0 = \partial_z U - u_*^2/\nu$, while η can be taken as a constant. Taking into account the functional form of (32) and

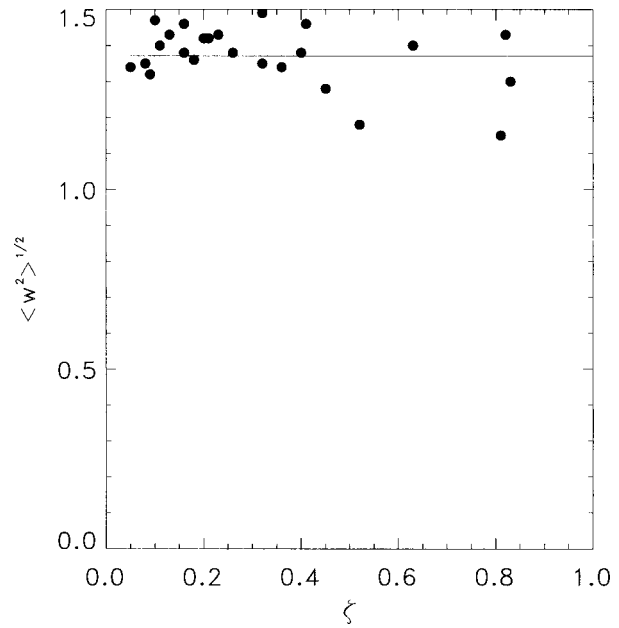

FIG. 9. Comparison of the constant theoretical prediction (line) with the Kansas observations (filled circles) for the $\langle w^2\rangle^{1/2}$ under stable conditions.

substitution into (15), leads (after proper nondimensionalization) to

$$\frac{\tilde{\eta}\tilde{U} + \tilde{\lambda}_0}{\partial_{\tilde{z}}\tilde{U}} = \tilde{z}, \qquad \frac{\tilde{\eta}\tilde{\Theta} + \tilde{\mu}_0}{\partial_{\tilde{z}}\tilde{U}} = \tilde{z}. \tag{33}$$

The most general solution of (33) is an algebraic law for both $\tilde{\Theta}$ and $\tilde{U}$; $\tilde{U} = \tilde{U}_1\tilde{z}^{1/\tilde{\eta}}$, leading to zero or infinite values for ϕ_u and ϕ_θ. The only way to obtain finite values, as observed in the atmosphere, is to let $\tilde{\eta} = 0$, in which case (33) yields $\phi_u = cte$ and $\tilde{\lambda}_0 = \tilde{\mu}_0$. Comparing (32) with $\eta = 0$ and with (12), we then get $\phi_\theta/\phi_u = cte$, and hence a constant value of ϕ_θ. This shows the limitation of our analysis; we can predict only shapes, and not absolute values, of the constants. The constants can be obtained only upon numerical implementation of our model.

4) Quantitative analysis: Stable case

In the case $\zeta > 0$ and $R_i \to 1/4$, the asymptotic expansion given in the appendix predicts that the ratio

$$\frac{\langle U\overline{w}\rangle}{\langle \overline{uw}\rangle} \approx \langle U\rangle(1 - 4R_i)^{1/2}\left(\frac{Lu_*}{k_*^2\nu}\right)^{1/2}\left(\frac{\phi_u}{\zeta}\right)^{1/2} N(\phi_u/\zeta), \tag{34}$$

where N is a numerical factor depending only on some constants and on ϕ_u/ζ. The ratio $\langle\Theta\overline{w}\rangle/\langle\overline{w\theta}\rangle$ also behaves exactly like (34), with a different numerical factor. So, for fixed L, these ratios approach zero as $R_i \to 1/4$ provided ϕ_u/ζ remains bounded. In that case, we have the natural ordering $\langle U\overline{w}\rangle \ll \langle\overline{uw}\rangle$ and $\langle\Theta\overline{w}\rangle \ll \langle\overline{\theta w}\rangle$, which confirms our physical expectation. In the previous section, we showed by qualitative arguments, that this ordering implies that $\phi_u \sim \zeta$ and $\phi_\theta \sim \zeta$. So, ϕ_u/ζ is bounded, which provides a consistency check of our asymptotic analysis.

Using the asymptotic expression, and the predominance of the subgrid stresses $\langle\overline{uw}\rangle$ and $\langle\overline{w\theta}\rangle$, one can also derive the fact that ϕ_u/ζ tends to a constant. For this, we use (21) to write

$$\frac{\langle\overline{uw}\rangle}{\langle\overline{w\theta}\rangle} = \frac{\zeta/\tilde{h}_u - 1}{\zeta/\tilde{h}_\theta - 1} \approx 1, \tag{35}$$

and then the asymptotic expansion yields

$$\frac{\langle\overline{uw}\rangle}{\langle\overline{w\theta}\rangle} = \frac{\lambda_1/4 + (\zeta/\phi_u)\lambda_2 + (\zeta/\phi_u)^2\lambda_3}{(\phi_u/\zeta)u_1/8 + \mu_2/4 + (\zeta/\phi_u)\mu_3/2}. \tag{36}$$

By equating (35) with (36), we see that ϕ_u/ζ is necessarily a constant, which depends on factors $\lambda_1, \ldots, \mu_3$. In fact, it is only our qualitative argument (now supported by the quantitative analysis), which can help us simplify the expression and write it only as a function of h_u/h_θ.

Quantitative analysis: Unstable case

In the case $\zeta \ll -1$ and $R_i \ll -1$, the asymptotic analysis predicts that $\langle U\overline{w}\rangle$ is proportional to $r_c = (2b - 2a)^{-1}(\partial_z U/\nu k_*^2)^{-(2a+1)/3}$, where a and b are functions of the Richardson number, and k_* is a characteristic horizontal wavenumber. In the same way, $\langle\overline{uw}\rangle$ is proportional to r_c^2 as is $\langle\overline{w\theta}\rangle$. On the other hand, in neutral conditions $R_i = 0$, $2a = -1$, $b = 0$, leading to $r_c = 1$. This suggests that we interpret r_c as a nondimensional correction to the surface "neutral" values of the friction velocity $u_*(R_i = 0)$ and $\theta_*(R_i = 0)$. In other words, this Richardson-dependent factor renormalizes the surface momentum and heat flux, and should disappear upon nondimensionalization of the velocities and of the temperatures by these quantities. Note that the condition that the renormalizing factor remain of order 1 even at $R_i \gg 1$ sets some conditions upon the characteristic wavenumber k_*, and hence our filtering procedure. Indeed, since $a \sim -(-R_i)^{1/2}$ for large R_i, we must have $k_*^2 \sim \partial_z U/\nu$ in order to avoid divergences of the surface fluxes. If ν is the molecular viscosity, this implies that k_* is of order $\mathrm{Re}^{-1/2}/d$, where Re is the Reynolds number of the flow. This implies taking a horizontal cutoff scale of the order of the Taylor scale of the flow (somewhere in the "middle" of the inertial range). If this scale appears too small to perform an efficient LES, one could still use our model, but at the price of introducing a "turbulent viscosity" $\nu_t = \partial_z U/k_*^2$ in place of ν, to efficiently damp the small scales. Such a procedure would not be surprising; if we choose our cutoff so large that the resolved scales are not dominant compared to the small scale then the local interactions become important even at subgrid scales. A way to remove them from the problem is to replace them by a turbulent eddy viscosity, modeling the action of the smallest scales onto the slightly larger (but still small) ones. This procedure has in fact been proposed as a way to generalize rapid distortion theory by Townsend (1976) and has recently been validated against direct numerical simulation of 3D homogeneous turbulence by Laval et al. (2001, manuscript submitted to *Phys. Fluids*).

After nondimensionalization by the surface fluxes and the scale L (the Monin–Obukhov scale), we expect the fluxes to behave like

$$\langle\tilde{U}\tilde{\overline{w}}\rangle = \frac{2(a-b)\zeta\tilde{U}}{\phi_u}\left(\frac{\zeta}{\phi_u}\eta_1 - 2b\eta_2\right),$$

$$\langle\tilde{\overline{w}}\tilde{\overline{u}}\rangle = \frac{\zeta}{\phi_u}\left[4b^2\lambda_1 + b\frac{\zeta}{\phi_u}\lambda_2 + \left(\frac{\zeta}{\phi_u}\right)^2\lambda_3\right],$$

$$\langle\tilde{\overline{w}}\tilde{\overline{\theta}}\rangle = \frac{\zeta}{\phi_u}\left(-8ab^2\frac{\phi_u}{\zeta}\mu_1 + 4ab\mu_2 - 2a\frac{\zeta}{\phi_u}\mu_3\right). \tag{37}$$

In the large–Richardson number limit, $a - b \sim a \sim b \sim -(-R_i)^{1/2}$. So, to leading order in R_i, the ratio $\langle\tilde{U}\tilde{\overline{w}}\rangle/\langle\tilde{\overline{w}}\tilde{\overline{u}}\rangle$ behaves like $\tilde{U}\eta_2/\lambda_1$ while the ratio $\langle\tilde{\Theta}\tilde{\overline{w}}\rangle/$

$\langle\widetilde{w\theta}\rangle$ varies as $\tilde{\Theta}\zeta/(\phi_u\sqrt{-R_i})$. The relative magnitude of these terms thus depends on both the magnitude of $\tilde{U}$ and $\tilde{\Theta}$, and upon the constants $\lambda_1, \ldots, \mu_3$ and the way ζ/ϕ_u varies with R_i. Since $\tilde{U}$ decreases under very unstable conditions, it is conceivable that for large enough R_i, the ratio $\langle\tilde{U}\widetilde{w}\rangle/\langle\widetilde{w}\tilde{u}\rangle$ eventually becomes less than one, while we predict that ϕ_u and ϕ_θ behave in such a way that $\langle\tilde{\Theta}\widetilde{w}\rangle/\langle\widetilde{w}\theta\rangle$ stays large at large $-R_i$.

Given this a priori estimate, we can now substitute into (30) the asymptotic expansion (37). From the first equation, and leaving aside numerical prefactors, we get

$$\frac{R_i\zeta}{\phi_u} \sim \zeta \sim \frac{\zeta^2\phi_\theta}{\phi_u^3}. \tag{38}$$

From the second one, we obtain the differential equation:

$$\frac{\tilde{\Theta}R_i\zeta}{\phi_u} \sim 1 \sim \frac{\partial_\zeta(\tilde{\Theta}^2)}{(\partial_\zeta\tilde{U})^3}. \tag{39}$$

The solution to the coupled system (38) and (39) is

$$\tilde{\Theta} = \tilde{\Theta}_0 + \frac{\tilde{\Theta}_1}{\zeta}, \qquad \phi_\theta \sim \frac{1}{\zeta}, \qquad \phi_u \sim cte. \tag{40}$$

We recover here the constancy of ϕ_u inferred from qualitative arguments. Neither this behavior, nor the asymptotic behavior of $\tilde{\Theta}$ and ϕ_θ is consistent with the ''free convection'' scaling $\tilde{\Theta} \sim \phi_\theta \sim \phi_u \sim \zeta^{-1/3}$ inferred from Prandtl's similarity theory. In fact, the dependence we find here is exactly that predicted by the theory of Malkus (Malkus 1954a,b), which seems to be in better agreement with experiments of large–Rayleigh number convection (Townsend 1959). Malkus's prediction follows from a maximum principle while our prediction follows from an asymptotic analysis of the Boussinesq equations. It is interesting that these two different approaches lead independently to the same prediction. At this point, it is worth mentioning that Malkus's maximum principle applied to free shear flows leads to the logarithmic law of the wall (Malkus 1956). In the same way, our approach to the same problem also leads to the logarithmic law of the wall and thus the coincidence between the two approaches may not be accidental. For example, it might be that the extrememum principle is in some way equivalent to our nonlocality assumption. Note that the constant value of ϕ_u at large $-\zeta$ implies a logarithmic profile for the mean velocity in this limit. It was shown by Shraiman and Siggia (1990) that this dependence was sufficient to explain the hard turbulence regime, in which the Nusselt scaling with the Rayleigh number changes from a 1/3 to a 2/7 power law. At the present time, we cannot decide whether our theoretical prediction corresponds to a hard or soft turbulence regime.[4] In fact, our computations were made using a

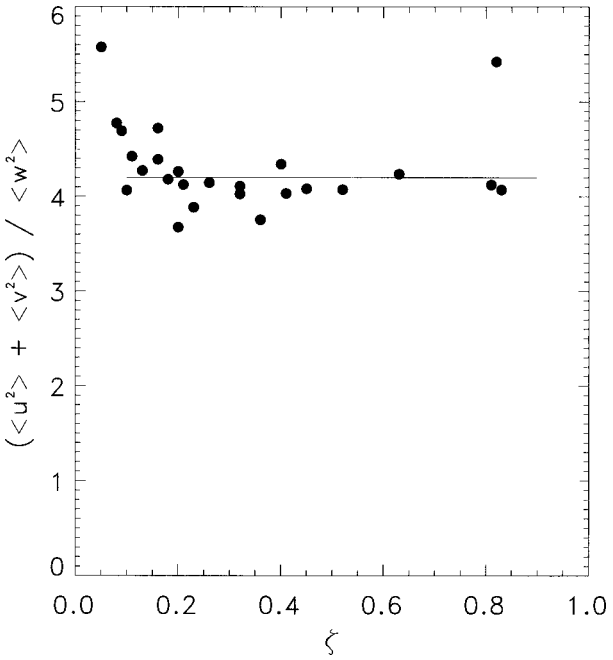

FIG. 10. Comparison of the constant theoretical prediction (line) with the Kansas observations (filled circles) for the $(\langle u^2\rangle + \langle v^2\rangle)/\langle w^2\rangle$ under stable conditions.

Prandtl number of 1, which according to the numerical two-dimensional results of Werne (1993) seems to be incompatible with the hard convection regime. It would then be interesting to generalize our computations to the case where Pr is much larger than one, to see whether different predictions arise for the structure of the surface layer. Finally, we may note that our prediction implies that asymptotically the Richardson number approaches a constant value, which seems to be a necessary condition for the boundary layer to be stabilized by the mean shear under hard turbulence conditions Castaing et al. (1989). This shows that the hard turbulence regime for the PSL cannot be ruled out, but we have no means to prove it.

From a practical point of view, it is worth checking whether the asymptotic prediction (40) can be supported by the available data on the atmospheric layer. Unfortunately, we were not able to find reliable data corresponding to $\zeta < -2$, so we are still far from any asymptotic regime. It is however easy to examine the simplest intermediate asymptotic regime compatible with (40) at large ζ and leading to a finite value of ϕ_u and ϕ_θ at $\zeta \to 0$. It is

$$\phi_u = \frac{1 + \alpha_1\zeta}{1 + \alpha_2\zeta}, \qquad \phi_\theta = \frac{\beta_1}{1 + \beta_2\zeta}. \tag{41}$$

The fit of these formula over the Kansas data, for the intermediate regime $-2 < \zeta < 0$ works extremely well (Figs. 5 and 6), showing that our theoretical prediction is not inconsistent with the available data.

[4] Here the terms ''hard'' and ''soft'' refer to the observed transition in the scaling exponent in the Nusslet versus Rayleigh number variation as in Castaing et al. (1989).

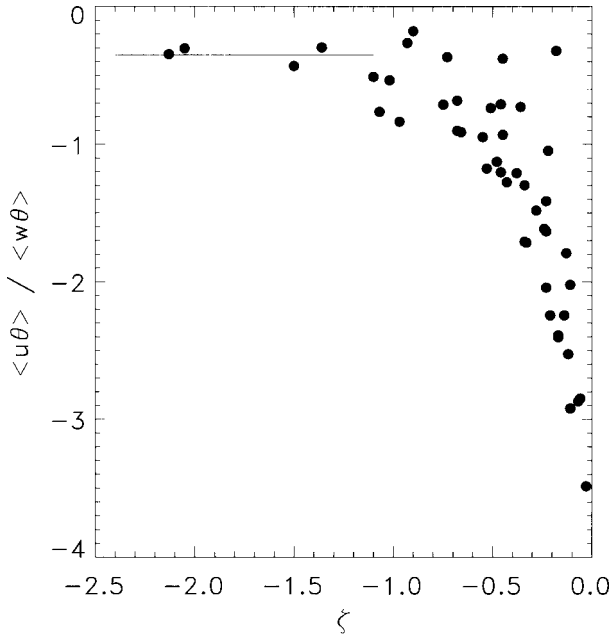

FIG. 11. Comparison of the constant theoretical prediction (line) with the Kansas observations (filled circles) for the $\langle u\theta\rangle/\langle w\theta\rangle$ under unstable conditions.

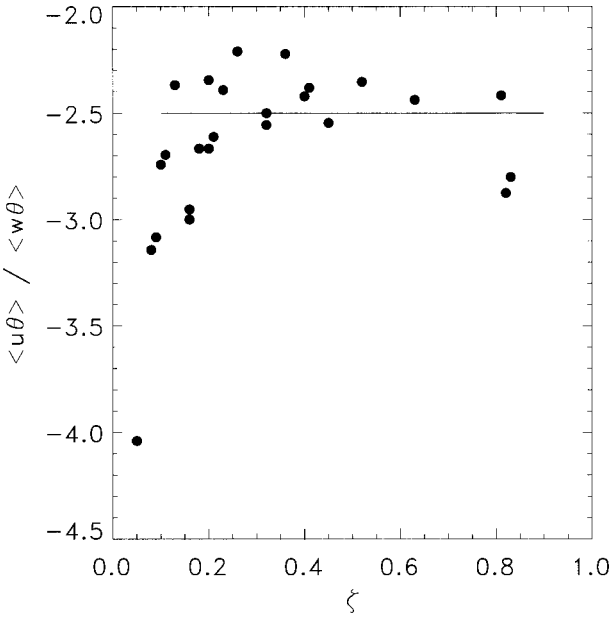

FIG. 12. Comparison of the constant theoretical prediction (line) with the Kansas observations (filled circles) for the $\langle u\theta\rangle/\langle w\theta\rangle$ under stable conditions.

c. Velocity and temperature variances

The results obtained in the previous sections and in the appendix can be used to derive expressions for the velocity and temperature variances, as a function of the stability of the layer. Indeed, from the equations for u and w as a function of the vorticity [Eq. (A1)], it is easy to see that the asymptotic expansion of $\langle u^2\rangle$ and $\langle w^2\rangle$ as a function of the Reynolds number, will be similar (same structure but different constants) to that of $\langle uw\rangle$, within a factor $(\partial_z U/\nu k_*^2)^{-1/3}$ accounting for some extra R dependence. To avoid divergences, we have tuned this factor to be unity. In the unstable case, we may thus use directly the expression of $\langle uw\rangle$ provided in the appendix [Eq. (A20)] to get, for large R_i,

$$\langle u^2\rangle \sim \langle w^2\rangle \sim \frac{1}{\partial_z U} \sim \frac{\zeta}{\phi_u}. \tag{42}$$

Since in this regime ϕ_u tends to a constant, we get a $\zeta^{1/2}$ behavior for the velocity variances in the unstable regime. This is different from the classical $\zeta^{1/3}$ prediction (free-fall regime), but it is not inconsistent with the present data, as illustrated in Fig. 7 for the vertical velocity. Taking into account the rather modest values of ζ, we may proceed as for the mean profiles and try to fit the data by a simple intermediate asymptotic regime compatible with (42); that is,

$$\langle w^2\rangle^{1/2} = \alpha_1 + \alpha_2\zeta^{1/2}. \tag{43}$$

This functional form applied to the Kansas data works extremely well for the vertical velocity, as shown in Fig. 7. For the horizontal velocity, a similar fit is still good, but since the scatter of the data is larger, the agreement is less significant. Note however that for $\zeta \ll -1$, the ratio of the horizontal velocity $u^2 + v^2$ to the vertical velocity w^2 indeed tends to a constant in the Kansas data (Fig. 8), as predicted by our model. In the stable regime, we may also use the expression of

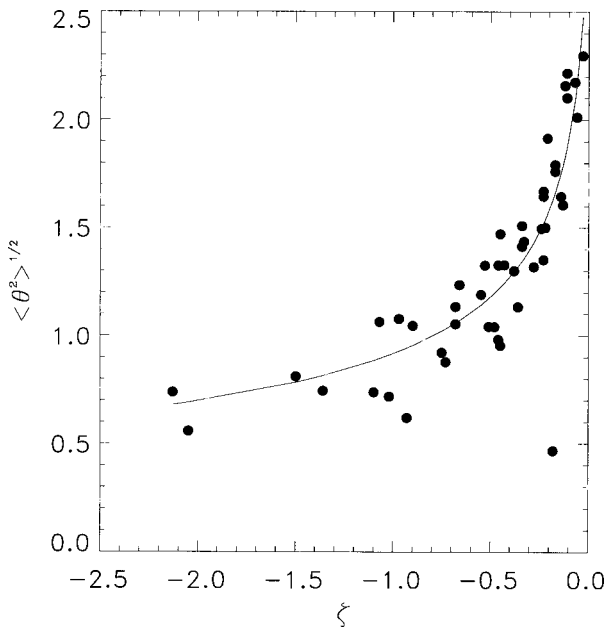

FIG. 13. Comparison of the theoretical prediction $\langle\theta^2\rangle^{1/2} \sim 1/(\alpha_1 + \alpha_2\zeta^{1/2})$ (line) with the Kansas observations (filled circles) for the temperature under unstable conditions. The best agreement is obtained with $\alpha_1 = 0.26$ and $\alpha_2 = 0.83$.

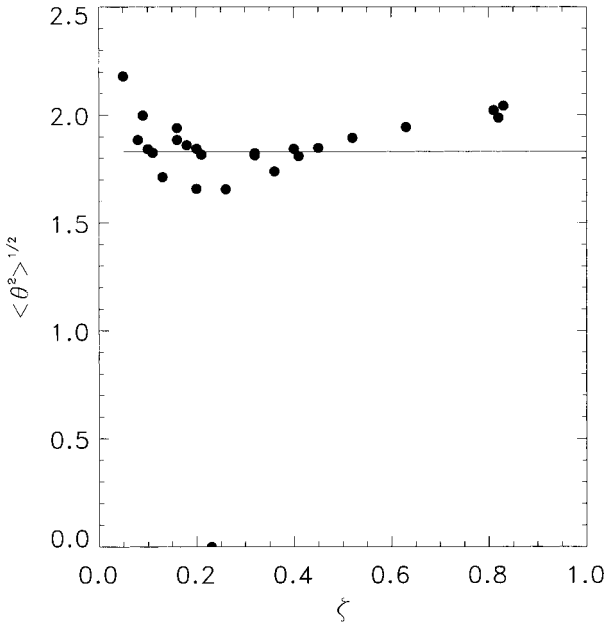

FIG. 14. Comparison of the constant theoretical prediction (line) with the Kansas observations (filled circles) for the temperature under stable conditions.

$\langle\overline{wu}\rangle$ provided in appendix, with $a \to b \to -1/4$, and take into account that in this limit, $\lambda_1, \ldots, \lambda_3 \to (a - b)^2\ln(\partial_z U/\nu k_*^2)$, thereby avoiding divergences. Given that in the stable regime, $\partial_z U \sim \phi_u/\zeta \sim cte$, we thus find that

$$\langle w^2\rangle \sim \langle u^2\rangle \sim cte, \tag{44}$$

in the stable regime. Again, this prediction is well satisfied by the vertical velocity variances, see Fig. 9. For u^2, again, the scatter is large, but the Kansas data are consistent with a constant ratio $u^2 + v^2/w^2$ at large ζ (Fig. 10), as predicted by our model. Similar arguments lead us to consider that the functional properties of the flux $\langle u\theta\rangle$ are similar to those of $\langle w\theta\rangle$. Using the expression of $\langle\overline{w\theta}\rangle$ provided in the appendix, we thus find in the unstable regime (large R_i), $\langle\overline{u\theta}\rangle$ obeys

$$\langle\overline{u\theta}\rangle \sim \sqrt{R_i} \sim cte. \tag{45}$$

In the stable regime, it is a function only of $\partial_z U$ and, thus, is constant. Given the large scatter of the data, a good indirect way of testing these predictions is to plot the ratio $\langle u\theta\rangle/\langle w\theta\rangle$ as observed in the Kansas data. Both for the unstable (Fig. 11) and the stable case (Fig. 12), we observe a trend toward constancy for large values of ζ, in agreement with the model. For the temperature fluctuations, the developments provided in the appendix can be repeated to give in the unstable case:

$$\langle\overline{\theta^2}\rangle \sim R_i\frac{\partial_z U^2}{g\beta} \sim R_i\frac{\phi_u}{\zeta} \sim \frac{1}{\zeta}, \tag{46}$$

while in the stable case, we get, similar to the velocity variances, $\langle\overline{\theta^2}\rangle \sim cte$. The comparison with the Kansas data is provided in Fig. 14. The unstable case (Fig. 13, the asymptotic intermediate formula $\langle\theta^2\rangle^{1/2} \sim 1/(\alpha_1 + \alpha_2\zeta^{1/2})$ provides an excellent fit of the data, while the constancy of $\langle\theta^2\rangle^{1/2}$ in the stable case also seems consistent with the data.

5. Summary

In this paper, we have used a new model for the atmospheric surface layer. This model involves the coupling of two dynamical equations; one for the large (resolved) scales of motions and another for the small (subgrid) scale velocity. The equations are coupled through resolved–subgrid and subgrid–subgrid interactions. The subgrid-scale equation is a linear inhomogeneous equation, where the forcing occurs via the energy and heat cascade from resolved to subgrid scale. Under the assumption of delta-correlated forces, the subgrid equation can be formally integrated, leading to an expression for the subgrid-scale velocity as a function of the resolved motions only. Again, this expression involves no adjustable parameters. In the present paper, we have used this analytic expression to study some physical properties of the atmospheric surface layer, such as the variation of the integral scale of the vertical motions, and the mean temperature and velocity profiles. For the vertical length scale, we found an estimate that is in good agreement with the Kansas observations (Wyngaard and Coté 1971). For the mean velocity and temperature profiles, we predict different behavior depending on stability $\zeta = z/L$, where L is the Monin–Obukhov length and z is the vertical coordinate; in the stable case, our model predicts that the nondimensional stability functions for momentum ϕ_u and heat ϕ_θ vary linearly with ζ in agreement with observations. In the unstable case, the model predictions of ϕ_u tend to a constant value for large $-\zeta$, while ϕ_θ behaves like $1/\zeta$. This behavior was shown to be compatible with the Kansas data and is in agreement with a theoretical prediction of Malkus (1954a,b) based on an extremum principle. For the temperature and velocity variances, we find that they should tend to a constant in the stable case. In the unstable case, our prediction is that the temperature variances should scale like $\zeta^{-1/2}$, and the velocity variances like $\zeta^{1/2}$. This prediction is in contradiction with the predictions of the free convection regime, but they are shown to be compatible with the Kansas observations.

These results show that some features of the atmospheric surface layer can be explained directly using the Navier–Stokes equations, and independently of any dimensional arguments. This also shows that our model, derived from the basic equations via a physical approximation, has the correct symmetry and asymptotic requirements built in, which is not necessarily the case of traditional subgrid modeling. The next step is to implement a full numerical model (resolved plus subgrid equations), in order to see whether quantitative agree-

ment can be reached via the consistent computation of the constants appearing in our analytic solutions. This is the subject of an ongoing work, which will be reported in future publications.

Acknowledgments. We thank Eun-Jin Kim for interesting discussions and for pointing us to the hypergeometrical solution of (A4) and Bernard Legras for a careful reading of the manuscript and for making many suggestions and corrections. John Wyngaard pointed out an inconsistence in a previous version of the manuscript. Partial funding for BD was provided by a NATO fellowship and PPS was supported under the ONR CBLAST Initiative N00014-00-C-0180. NCAR is sponsored by the National Science Foundation.

APPENDIX

Analytical Developments

a. Analytical solutions of small-scale equation

In this appendix, we develop the analytic solution to the system of ray equations (4). For convenience, we first introduce the vorticity:

$$\hat{\omega} = iq\hat{u} - ik\hat{w}, \qquad \hat{u} = \frac{-iq}{k^2 + q^2}\hat{\omega},$$

$$\hat{w} = \frac{ik}{k^2 + q^2}\hat{\omega}. \tag{A1}$$

Then, solving for $\hat{u}$ and $\hat{w}$ is equivalent to solving for $\hat{\omega}$. Combining the ray equations (4), we then find the coupled system for $\hat{\omega}$ and $\hat{\theta}$:

$$D_R\hat{\omega} = +ik\frac{g\beta}{\partial_z U}\hat{\theta} + \frac{\nu k^2}{\partial_z U}(1 + R^2)\hat{\omega} - \frac{\hat{F}_\omega}{\partial_z U},$$

$$D_R\hat{\theta} = +\frac{i}{k}\frac{\partial_z\Theta}{\partial_z U}\left(\frac{\hat{\omega}}{1 + R^2}\right) + \frac{\kappa k^2}{\partial_z U}(1 + R^2)\hat{\theta} - \frac{\hat{F}_\theta}{\partial_z U}, \tag{A2}$$

where $\hat{F}_\omega = iq\hat{F}_u^\perp - ik\hat{F}_w^\perp$.

To solve this system of equations, we first solve the homogeneous system (i.e., with $F_\omega = F_\theta = 0$) under the approximation $\kappa = \nu$ (Prandtl number Pr = 1). Note that by introducing

$$\omega^\dagger = \omega \exp\left[\frac{\nu k^2}{\partial_z U}\left(-R - \frac{R^3}{3}\right)\right],$$

$$\theta^\dagger = \theta \exp\left[\frac{\nu k^2}{\partial_z U}\left(-R - \frac{R^3}{3}\right)\right], \tag{A3}$$

we can eliminate the viscous terms from the homogeneous equations. Combining the resulting equations, leads to a second-order equation for $\omega^\dagger$, of the form:

$$D_{R^2}^2\omega^\dagger = -R_i\frac{\omega^\dagger}{1 + R^2}. \tag{A4}$$

where R_i is the Richardson number defined by

$$R_i = \frac{g\beta\partial_z\Theta}{(\partial_z U)^2}. \tag{A5}$$

By the transformation $x = 1 + R^2$, this equation can be put in the form of a Gauss' differential equation:

$$x(1 - x)d_{x^2}^2\omega^\dagger + [c - (a + b + 1)x]d_x\omega^\dagger - ab\omega^\dagger = 0, \tag{A6}$$

with

$$c = 0, \qquad a = -\frac{1}{4}[1 + (1 - 4R_i)^{1/2}],$$

$$b = -\frac{1}{4}[1 - (1 - 4R_i)^{1/2}]. \tag{A7}$$

These coefficients are real for $R_i < 1/4$ (unstable case) and have an imaginary part for $R_i > 1/4$ (stable case), inducing oscillations of the solution.

Two independent solutions of this equation are ${}_2F_1(a, b, c, x)$ and $x^{1-c}{}_2F_1(1 + a - c, 1 + b - c, 2 - c, x)$. Their asymptotic behavior for large x is algebraic, like $x^{\max(-a,-b)}$. In terms of the original variables, this means that the two independent solutions for ω are

$$\omega_1 = {}_2Fk_1(a, b, 0, 1 + R^2)\exp\left[\frac{\nu k^2}{\partial_z U}\left(-R - \frac{R^3}{3}\right)\right],$$

$$\omega_2 = (1 + R^2)\,{}_2F_1(1 + a, 1 + b, 2, 1 + R^2) \times \exp\left[\frac{\nu k^2}{\partial_z U}\left(-R - \frac{R^3}{3}\right)\right], \tag{A8}$$

which are viscously damped solutions for $R < 0$. The associated solution for θ is obtained by replacing ω by ω_1 or ω_2 in the first equation of (A2). We call $\boldsymbol{\phi}_1 = (\omega_1, \theta_1)$ and $\boldsymbol{\phi}_2 = (\omega_2, \theta_2)$ the corresponding couples of the independent solutions. Now, we introduce the 2×2 matrix $\mathbf{K}(R)$ with columns $\boldsymbol{\phi}_1$ and $\boldsymbol{\phi}_2$. We also introduce the vector $\mathbf{F} = (F_\omega, F_\theta)$. The general solution of the inhomogeneous system (A2) can then be written as

$$\boldsymbol{\phi}(R) = \mathbf{K}(R)\mathbf{K}^{-1}(R_0)\boldsymbol{\phi}_0 + \mathbf{K}(R)\int_{R_0}^{R}\mathbf{K}^{-1}(r)\mathbf{F}(r)\,dr. \tag{A9}$$

Taking as initial condition $\phi = 0$ at $R_0 = -\infty$ (no small scales at $t = -\infty$), we can finally write the general solution as

$$\boldsymbol{\phi}(R) = \int_{-\infty}^{R} \mathbf{K}(R)\mathbf{K}^{-1}(r)\mathbf{F}(r)\, dr. \qquad \text{(A10)}$$

Note that the integrand is just the solution of the homogeneous system, with initial condition $\boldsymbol{\phi}(R = r) = \mathbf{F}(r)$. This point is used in section 4. Also, consider a product of two components of ϕ, say $\phi_\omega \phi_\omega^* = |\hat{\omega}|^2$. Upon using (A10), we can write

$$|\hat{\omega}|^2 = \sum_{j,l,j',l'=1}^{2} \int_{-\infty}^{R} dr_0 \int_{-\infty}^{R} dr_1 K_{1j}(R)K_{1j'}^*(R)K_{jl}(r_0)K_{j'l'}^*(r_1)F_l(r_0)F_{l'}^*(r_1). \qquad \text{(A11)}$$

Now, suppose that we take a time average of a quantity involving $|\hat{\omega}|^2$. Because of the delta correlations of the force, the average brings down a factor $|\partial_z U|\,\delta(r_1 - r_0)$ [because $t - t_0 = -\partial_z U(R - R_0)$], and so Eq. (A11) will simply look, after integration over say, r_1 as

$$\langle |\hat{\omega}|^2 \rangle = |\partial_z U| \int_{-\infty}^{R} dr_0 \sum_{j,l,j',l'=1}^{2} K_{1j}(R)K_{1j'}^*(R)K_{jl}(r_0)K_{j'l'}^*(r_0)\langle F_l(r_0)F_{l'}^*(r_0)\rangle. \qquad \text{(A12)}$$

Here, the integrand of (A.12) is just the product of two solutions of the homogeneous system with initial condition $\phi(R = r) = \mathbf{F}(r)$. This point is also used in section 4. We stress once more that this simplification is only valid when one performs the averaging procedure.

b. Asymptotic expansions of the solutions as a function of R_i

To determine the mean velocity and temperature profiles, it is necessary to find an approximation of the solution of (A4) at large R. In that limit, the equation (A4) becomes in normal variables

$$D_R^2\hat{\omega} = -R_i\frac{\hat{\omega}}{R^2} + \frac{\nu k^2}{\partial_z U}R^2\hat{\omega}, \qquad \text{(A13)}$$

where the two independent solutions are

$$\hat{\omega}_1 = R^{-2a}e^{\nu k^2 R^3/(3\partial_z U)}, \qquad \hat{\omega}_2 = R^{-2b}e^{\nu k^2 R^3/(3\partial_z U)}, \qquad \text{(A14)}$$

with a and b given in (A7). Using these solutions, one may then write the matrix $\mathbf{K}(R)$ in terms of a Green's function as

$$\mathbf{K}(R) = \begin{pmatrix} R^{-2a} & R^{-2b} \\ \dfrac{\partial_z U}{igk\beta}2aR^{-2a-1} & \dfrac{\partial_z U}{igk\beta}2bR^{-2b-1} \end{pmatrix} e^{\nu k^2 R^3/(3\partial_z U)}, \qquad \text{(A15)}$$

whose inverse is

$$\mathbf{K}^{-1} = \begin{pmatrix} \dfrac{b}{b-a}R^{2a} & -\dfrac{igk\beta}{2(b-a)\partial_z U}R^{1+2a} \\ -\dfrac{a}{b-a}R^{2b} & \dfrac{igk\beta}{2(b-a)\partial_z U}R^{1+2b} \end{pmatrix} e^{-\nu k^2 R^3(3\partial_z U)}. \qquad \text{(A16)}$$

Using these expressions and the representation (A10), we can finally write an approximate expression for $\hat{\omega}$ and $\hat{\theta}$, valid at large R and R_0:

$$\hat{\omega} = \frac{1}{2\partial_z U(a-b)}\int_R^\infty dR_0 \left\{ \left[2b\left(\frac{R}{R_0}\right)^{-2a} - 2a\left(\frac{R}{R_0}\right)^{-2b} \right] F_\omega(k, R_0) - \frac{igk\beta}{\partial_z U}R_0 \left[\left(\frac{R}{R_0}\right)^{-2a} - \left(\frac{R}{R_0}\right)^{-2b} \right] F_\theta(k, R_0) \right\} e^{\nu k^2 (R-R_0)^3/(3\partial_z U)}$$

$$\hat{\theta} = \frac{1}{2\partial_z U(b-a)}\int_R^\infty dR_0 \left\{ \frac{\partial_z U}{igk\beta}\frac{4ab}{R} \left[\left(\frac{R}{R_0}\right)^{-2b} - \left(\frac{R}{R_0}\right)^{-2a} \right] F_\omega(k, R_0) + \left[2a\left(\frac{R}{R_0}\right)^{-2a-1} - 2b\left(\frac{R}{R_0}\right)^{-2b-1} \right] F_\theta(k, R_0) \right\}$$

$$\times\, e^{\nu k^2 (R-R_0)^3/(3\partial_z U)}. \qquad \text{(A17)}$$

Here, we have approximated $R^3 - R_0^3$ by $(R - R_0)^3$.

c. Asymptotic expansion of the subgrid stresses as a function of Reynolds number

Here, we would like to find an asymptotic expression for the subgrid velocity $\overline{w}$ and subgrid stresses $\overline{uw}$ and $\overline{w\theta}$ as a function of $\partial_z U$ and R_i. To do that, we note that the solutions (A17) behave algebraically like R^{-2a} or R^{-2b} at large R, and so, the corresponding subgrid stresses, which imply an integration over R up to infinity diverge in the limit $\nu \to 0$. So the viscosity acts here as a regularization factor, preventing unbounded growth. This shows that an expansion in the small parameter ν (or in nondimensional units, 1/Re, where Re is some Reynolds number) will capture the leading order behavior of the subgrid stresses. In the atmosphere, the Reynolds number is quite large, so it can be expected that even the first-order term will give a very good approximation.

To find this expansion, we use the expression (10) and (14) to express the subgrid stresses as a function of $\hat{\omega}$ and $\hat{\theta}$. Interchanging the integration in R and R_0, and using the expression (A17), we get, for example,

$$\overline{w} = -\frac{i}{2\partial_z U(a-b)} \int \frac{dk}{k} \int dR_0 \int_{-\infty}^{R_0} dR \times \left\{ \left[2b\left(\frac{R}{R_0}\right)^{-2a} - 2a\left(\frac{R}{R_0}\right)^{-2b} \right] F_\omega(k, R_0) - \frac{igk\beta}{\partial_z U} R_0 \left[\left(\frac{R}{R_0}\right)^{-2a} - \left(\frac{R}{R_0}\right)^{-2b} \right] F_\theta(k, R_0) \right\} \times e^{\nu k^2 (R-R_0)^3/(3\partial_z U)}. \quad \text{(A18)}$$

Now make the change of variable $R \to R_0 - \xi\alpha^{-1/3}$, where $\alpha = k_*^2\nu/\partial_z U \sim 1/\mathrm{Re}$ is a small parameter. Here, k_* is a typical horizontal wavenumber (of the order of the inverse of the horizontal cutoff scale). The leading order in the expansion of $\langle w \rangle$ in α will then be given by the power law with the largest exponent in R. From the expression of a and b in (A7), one can check that $-2a$ always dominates, for any R_i. Performing the change of variable, and collecting terms, we finally find to leading order in α that

$$\langle U\overline{w} \rangle = \langle U \rangle \frac{1}{2\partial_z U(a-b)} \left(\frac{\partial_z U}{\nu k_*^2} \right)^{-(1+2a)/3} \left(\frac{g\beta}{\partial_z U} \eta_1 - 2b\eta_2 \right), \quad \text{(A19)}$$

where k_* is a typical horizontal wavenumber (of the order of the inverse cutoff length) and η_1 and η_2 are two constant parameters depending only on complicated integrals of F_w and F_θ over k and R_0. Proceeding along the same line for $\langle \overline{uw} \rangle$ and $\langle \overline{w\theta} \rangle$, we find their leading order as

$$\langle \overline{wu} \rangle = \frac{1}{2\partial_z U(a-b)^2} \left(\frac{\partial_z U}{k_*^2 \nu} \right)^{-(2+4a)/3} \times \left[4b^2\lambda_1 + \frac{g\beta}{\partial_z U} b\lambda_2 + \left(\frac{g\beta}{\partial_z U} \right)^2 \lambda_3 \right],$$

$$\langle \overline{w\theta} \rangle = \frac{1}{2\partial_z U(a-b)^2} \left(\frac{\partial_z U}{k_*^2 \nu} \right)^{-(2+4a)/3} \times \left(-8ab^2 \frac{\partial_z U}{g\beta} \mu_1 + 4ab\mu_2 - 2a \frac{g\beta}{\partial_z U} \mu_3 \right). \quad \text{(A20)}$$

Comparing (A19) and (A20), with (11), (12), and (14), one can find expressions for λ, μ, and η as a function of R_i and $\partial_z U$. Note that in this appendix, velocities and temperature have not been nondimensionalized. We discuss in section 4b(5) how to nondimensionalize them, and this renormalization effects some factors in (A20) and (A19).

REFERENCES

Castaing, B., and Coauthors, 1989: Scaling of hard thermal turbulence in Rayleigh-Bénard convection. *J. Fluid Mech.*, **204,** 1–30.

Caughey, S. J., J. C. Wyngaard, and J. C. Kaimal, 1979: Turbulence in the evolving stable boundary layer. *J. Atmos. Sci.*, **36,** 1041–1052.

Dubrulle, B., 2000: Scaling laws prediction from a solvable model of turbulent convection. *Europhys. Lett.*, **51,** 513–519.

——, J-P. Laval, S. Nazarenko, and N. Kevlahan, 2001: Derivation of mean equilibrium profiles in plane parallel geometry using a new dynamical subgrid model. *Phys. Fluids*, **13,** 2045–2064.

——, ——, P. P. Sullivan, and J. Werne, 2002: A new dynamical subgrid model for the planetary surface layer. Part I: The model and a priori tests. *J. Atmos. Sci.*, **59,** 861–876.

Kaimal, J. C., J. C. Wyngaard, Y. Izumi, and O. R. Coté, 1972: Spectral characteristics of surface layer turbulence. *Quart. J. Roy. Meteor. Soc.*, **98,** 563–589.

Malkus, W. V. R., 1954a: Discrete transitions in turbulent convection. *Proc. Roy. Soc. London*, **225A,** 185–195.

——, 1954b: The heat transport and spectrum of thermal turbulence. *Proc. Roy. Soc. London*, **225A,** 195–212.

——, 1956: Outline of a theory of turbulent shear flow. *J. Fluid Mech.*, **1,** 521–539.

Nazarenko, S., 2000: On exact solutions for near wall turbulence theory. *Phys. Lett. A*, **264,** 444–448.

——, N. Kevlahan, and B. Dubrulle, 2000: Nonlinear RDT theory of near wall turbulence. *Physica D*, **138,** 158–176.

Shraiman, B. I., and E. D. Siggia, 1990: Heat transport in high-Rayleigh number convection. *Phys. Rev. A.*, **42,** 3650–3654.

Tong, C., J. C. Wyngaard, and J. G. Brasseur, 1999: Experimental study of the subgrid-scale stresses in the atmospheric surface layer. *J. Atmos. Sci.*, **56,** 2277–2292.

Townsend, A. A., 1976: *The Structure of Turbulent Shear Flow*. 2d ed. Cambridge University Press, 429 pp.

Townsend, J. J., 1959: Temperature fluctuations over a heated horizontal surface. *J. Fluid Mech.*, **5,** 209–241.

Werne, J., 1993: Structure of hard-turbulent convection in two dimensions: Numerical evidence. *Phys. Rev. E*, **48,** 1020–1035.

Wyngaard, J. C., and O. R. Coté, 1971: The budgets of turbulent kinetic energy and temperature variance in the atmospheric surface layer. *J. Atmos. Sci.*, **28,** 190–201.